

# Microstructural Changes and Volatilization of Rh and Rh/Ce on SiO<sub>2</sub> and Al<sub>2</sub>O<sub>3</sub> in NO + CO<sup>1</sup>

K. R. KRAUSE<sup>2</sup> AND L. D. SCHMIDT

*Department of Chemical Engineering and Materials Science, University of Minnesota, Minneapolis, Minnesota 55455*

Received August 25, 1992; revised November 3, 1992

Dramatic changes in the microstructures of Rh and Rh/Ce supported on SiO<sub>2</sub> and Al<sub>2</sub>O<sub>3</sub> occur after treatments in NO + CO at temperatures as low as 300°C. Silica-supported Rh was nearly completely volatilized by treatment in NO + CO at 300°C, but the addition of Ce was found to retard this effect. Examination of the effects of the individual gases showed that NO alone disperses Rh over the SiO<sub>2</sub> and CO alone volatilizes the dispersed Rh formed by treatment in NO. However, heating in CO alone had no effect on undispersed Rh. The activity of Rh on porous SiO<sub>2</sub> for NO + CO at 200°C decreased by a factor of five after heating overnight at 300°C due to loss of Rh. On alumina, heating in NO + CO had much less effect and only a few smaller particles disappeared even after extensive treatment at 400°C. Heating in NO alone, however, did disperse the Rh into small (~20 Å) particles on the Al<sub>2</sub>O<sub>3</sub>. Similar changes were observed for Rh/Ce. The NO + CO activity on alumina actually increased slightly by heating at 300°C for extended time. XPS indicates the presence of small amounts of oxidized Rh on both supports after heating in NO + CO, but cannot identify whether this is the dispersed Rh or the oxidized surface of Rh particles. We speculate that dispersion may be through the formation of a mobile nitrosyl complex and volatilization by formation of volatile carbonyls. © 1993 Academic Press, Inc.

## INTRODUCTION

Rh and Ce are used to remove NO and CO from exhaust in the automotive catalyst. Rh is the metal primarily responsible for NO<sub>x</sub> removal, and Ce addition has been shown to have beneficial effects on catalyst performance. While Ce is generally inactive, Ce addition to Rh improves selectivity and rate of CO + NO on alumina (1, 2), improves oxygenate selectivity (3) and the rate (4) of CO hydrogenation, but has little effect on ethane hydrogenolysis activity (4). The dispersion of Rh on SiO<sub>2</sub> measured by H<sub>2</sub> chemisorption was increased by Ce addition, but no effect was observed on Al<sub>2</sub>O<sub>3</sub> (2).

We have previously characterized the microstructure of Rh/Ce on SiO<sub>2</sub> (5) and Al<sub>2</sub>O<sub>3</sub>

(6) in oxidizing and reducing environments using TEM, HREM, EELS, and XPS. On SiO<sub>2</sub>, Ce was transformed between Ce<sup>+3</sup> in H<sub>2</sub> and CeO<sub>2</sub> in O<sub>2</sub>, and Rh dispersion was significantly altered by this heating cycle. However, on Al<sub>2</sub>O<sub>3</sub> heating in H<sub>2</sub> did not reduce the Ce from CeO<sub>2</sub>, and the Rh particles were immobile. All the treatments studied in previous work were at relatively high temperatures (>600°C) and under extreme conditions of pure H<sub>2</sub> or O<sub>2</sub> to simulate the effects on microstructure of long term exposures to actual reaction environments.

In this paper we have investigated the effects of treatment in NO and CO on the microstructure and reactivity of silica and alumina supported Rh and Rh/Ce. The NO + CO treatments studied here were at much lower temperatures, typically 300 to 400°C.

Before discussing the results, it is useful to review the effects of oxidation-reduction cycling on the microstructure of Rh on SiO<sub>2</sub>

<sup>1</sup> This research sponsored by the NSF under Grant CBT-882745 and by a grant from Ford Motor Company.

<sup>2</sup> Present address: Du Pont Chemicals, Experimental Station, Wilmington, DE 19880-0336.

(7) and  $\text{Al}_2\text{O}_3$  (6). After heating in  $\text{H}_2$ , highly faceted 100–200 Å diameter Rh metal particles form on the support. Heating in air at 500°C oxidizes the Rh to  $\text{Rh}_2\text{O}_3$ , and the particles assume rougher and slightly larger outlines as the oxide wets the silica. Heating in  $\text{H}_2$  at successively higher temperatures first reduces the  $\text{Rh}_2\text{O}_3$  back to many small metal crystals ( $\sim 300^\circ\text{C}$ ) which sinter into larger particles identical in size to the initial Rh particles ( $\sim 600^\circ\text{C}$ ). The interesting observations to compare with the results presented here are that (1) Rh particles are not mobile or volatile under these conditions and (2) the microstructure is unchanged after high-temperature oxidation–reduction cycling.

An interesting phenomenon which was first reported by Yang and Garland in the 1950s (8) and has received much attention lately from several groups (9–12) is the disruption of small Rh clusters on  $\text{SiO}_2$  or  $\text{Al}_2\text{O}_3$  into isolated Rh atoms by room-temperature treatment in CO. This has been inferred from IR, XPS, and EXAFS, but to our knowledge has not been directly observed. Indeed, detection of such small clusters by TEM is difficult, and disruption of larger particles does not occur due to energetic considerations. Solymosi has shown that addition of NO to CO greatly enhances the rate of disruption (13) and that Ce addition to Rh stabilizes the disrupted phase (14). However, increasing the temperature even to 100°C, hinders disruption since CO reduces the  $\text{Rh}^{\text{I}}$  gem-dicarbonyl formed by the isolated atoms. Catalytic disruption has some similarities to the transformations we report here, but several important differences exist. We observe dispersion of much larger Rh particles on  $\text{SiO}_2$  at realistic reaction temperatures by treatment in NO alone and their subsequent volatilization by treatment in CO. Significantly less volatilization was observed for Rh on  $\text{Al}_2\text{O}_3$ .

#### EXPERIMENTAL

TEM sample preparation has been described in detail elsewhere (4). About 200 Å

thick films of  $\text{SiO}_2$  or  $\text{Al}_2\text{O}_3$  were prepared by vacuum evaporating Si or Al onto formvar coated gold TEM grids and heating in  $\text{O}_2$  to decompose the formvar and oxidize the metal. Amorphous silica samples were prepared by heating at 800°C, and crystalline  $\gamma$ -alumina was prepared by heating at 600°C. About 20 Å films of Rh and Ce were vacuum evaporated on top of the support, and the grid was heated in  $\text{H}_2$  usually at 650°C to disperse the Rh film into 100–200 Å diameter particles. Ce wets the  $\text{SiO}_2$  and  $\text{Al}_2\text{O}_3$  except that some samples with  $\sim 100$  Å Ce formed interconnected island structures.

Several Rh/Ce ratios were prepared *on a single grid* by selectively shielding regions of the grid during evaporations. This ensured that multiple loadings prepared on the same grid received identical heat treatments. TEM was performed on a Philips CM30 (point-to-point resolution of 2.2 Å) and the same areas were examined repeatedly after successive treatments and transfer in air between the furnace and TEM. While exposure to air may affect the microstructure of very highly dispersed particles, no such evidence has been observed by this group in this and similar studies on 100–200 Å particles.

Reactivity measurements were performed on powder catalysts prepared by standard aqueous impregnation techniques. Appropriate amounts of  $\text{RhCl}_3 \cdot 3\text{H}_2\text{O}$  and  $\text{Ce}(\text{NO}_3)_3 \cdot 3\text{H}_2\text{O}$  solutions were added to Aerosil 200 silica (200  $\text{m}^2/\text{g}$ ) or Aesar  $\gamma$ -alumina (100  $\text{m}^2/\text{g}$ ), and the slurry was dried in  $\text{N}_2$  at 100°C overnight before calcining for 4 hr in  $\text{O}_2$ . Silica catalysts were calcined at 650°C and alumina catalysts at 500°C. About 200 mg of catalyst was placed in a Pyrex U-tube reactor, and activity was measured between 200 and 300°C.

Unless otherwise indicated, TEM sample treatments and reactivity measurements were made for 5% NO, 5% CO, and 5% NO + 5% CO from room temperature up to 500°C. The diluent was ultra-high purity He, and the CO was passed through a

molecular sieve trap to remove any metal carbonyls. Compositions of feed streams and products were determined by gas chromatography.

Samples for XPS were prepared and treated similarly to the TEM grids, except that an oxidized silicon wafer (with  $\sim 500$  Å of Al deposited on top for alumina samples) was used as the support. XPS was performed on a PHI 5400 spectrometer, and peak energies were referenced to adventitious carbon at 284.6 eV to correct for charging.

#### MICROSTRUCTURE

##### *Rh on SiO<sub>2</sub>*

*NO + CO.* The effects of successive treatments in NO + CO at 300°C on the microstructure of Rh on SiO<sub>2</sub> are shown in Fig. 1. After the initial treatment in H<sub>2</sub> at 650°C for 10 hr (Fig. 1a), Rh is present as  $\sim 150$  Å diameter metal particles and significant faceting is observed in many of the particles. Heating in NO + CO for 20 hr produced several changes in the microstructure (Fig. 1b). First, several smaller particles *disappeared*. Two such particles are indicated by vertical arrows in Figs. 1a and 1b. Second, a *lower contrast shell* has formed around the perimeters of many of the larger particles and the high contrast metal core has decreased in size. In most cases, the diameter of shell and core combined is unchanged from Fig. 1a. Finally, dispersion of Rh on the SiO<sub>2</sub> surface is also observed. One such area is indicated by horizontal arrows in Figs. 1a and 1b. Overall, the contrast of the Rh particles observed after treatment in NO + CO is lower than after H<sub>2</sub> treatment.

Figure 1c shows the microstructure of the same area after treatment for a longer time in NO + CO. All of the particles, even some as large as 300 Å in diameter, have disappeared leaving only faint outlines. Thus, the Rh has either been completely dispersed on the SiO<sub>2</sub> surface or has formed a volatile compound and evaporated. Figure 1d shows

the microstructure of the same area after heating in H<sub>2</sub> at 650° for 6 hr. A dispersed film of Rh would be expected to reform Rh particles by heating in H<sub>2</sub>, but only small ( $<50$ -Å diameter) particles are observed, and only sintering of nearby particles was observed after more extensive treatment in H<sub>2</sub>. The Rh loading has thus decreased dramatically by heating in NO + CO at only 300°C, and comparison of Fig. 1a with Fig. 1d shows that only about 5% of the Rh remains.

The only rings observed in electron diffraction patterns after each treatment in Fig. 1 were from fcc Rh metal and diffuse scattering from the amorphous SiO<sub>2</sub>. No Rh rings were observed after the second NO + CO treatment, but spotty rings returned after heating in H<sub>2</sub>. The low-contrast regions surrounding the Rh core and the dispersed Rh observed in Fig. 1b, however, may be either amorphous or too thin to detect.

Disappearance of Rh appears to occur faster for Rh<sub>2</sub>O<sub>3</sub> than for Rh metal. Figures 2a and 2b show the same area after first heating in O<sub>2</sub> at 600°C for 4 hr and then after heating in NO + CO at 300°C for 24 hr. Heating in O<sub>2</sub> oxidizes the Rh to Rh<sub>2</sub>O<sub>3</sub> as expected. After the single treatment in NO + CO, several of the smaller particles (indicated by arrows) have completely disappeared and the large particles have shrunk significantly while forming a wide shell around their perimeters. The 300 Å diameter particle in the right center, for example, has decreased to about half its original size, and a low-contrast ring is visible around its perimeter. Significantly more disappearance of Rh was observed on oxidized samples than on reduced samples after identical treatments.

*CO only.* No changes in microstructure other than slight sintering of adjacent Rh particles were observed after Rh samples were treated in CO (not shown); this was observed for extensive treatments at several different temperatures up to 500°C (including room temperature) and for treatment in pure CO. Even the smaller particles were

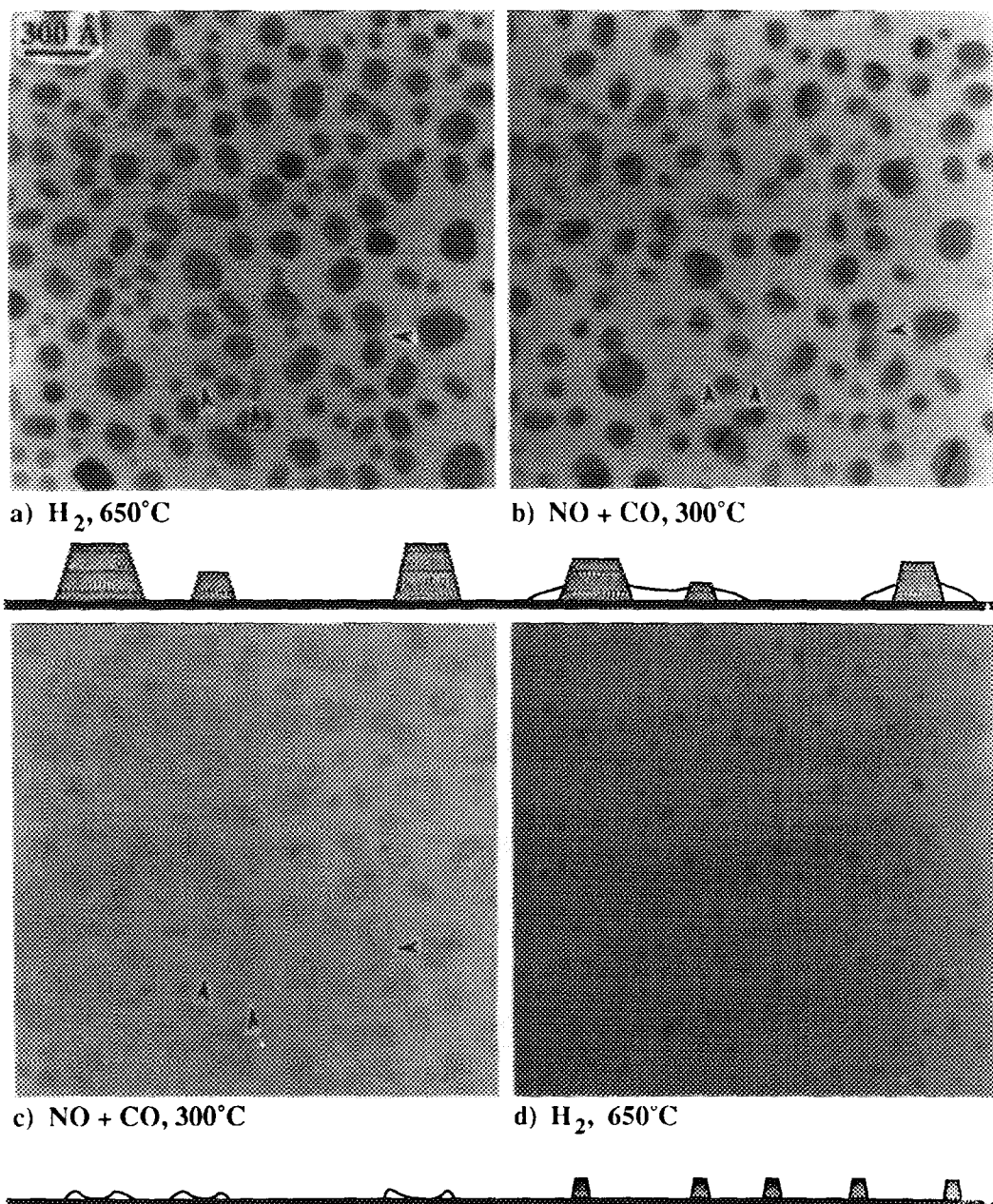
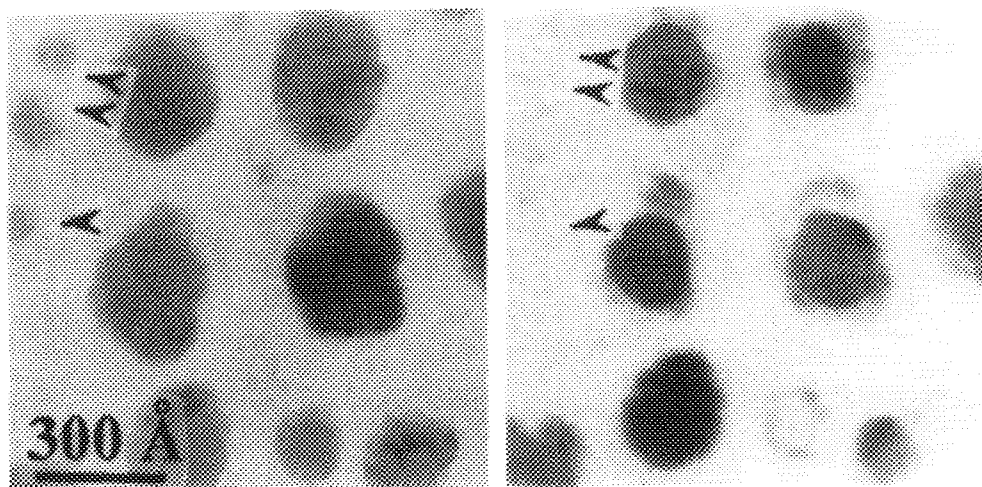


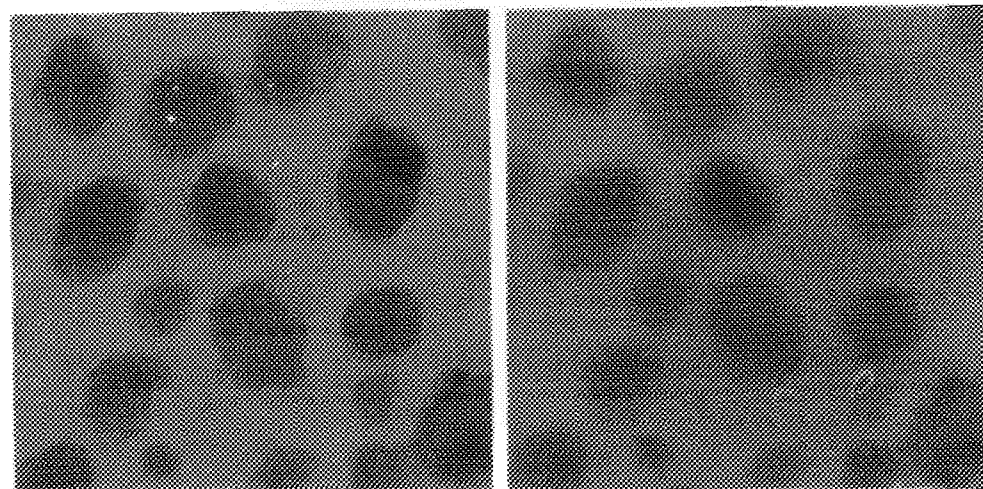
FIG. 1. Microstructure of Rh on  $SiO_2$  after heating in  $NO + CO$  at temperatures indicated. Vertical arrows indicate Rh particles which have disappeared after the first treatment, and the horizontal arrow indicates the area where Rh has dispersed on the  $SiO_2$ .

still observed after extensive heating in  $CO$ . No changes were observed in the diffraction patterns. Treatment in  $CO$  appears to have very little effect on the microstructure of Rh particles.

*NO only.* Figures 3a–3c illustrate the effect of heating in  $NO$  on the microstructure. Rh particles formed after the initial  $H_2$  treatment at  $650^\circ C$  for 10 hr are shown in Fig. 3a. The same particles are shown in Figs.

a) O<sub>2</sub>, 600°C

b) NO + CO, 300°C

c) O<sub>2</sub>, 600°C

d) NO, 400°C



FIG. 2. (a), (b) Microstructure of oxidized Rh after heating in NO + CO. Disappearance of Rh is greater than for similar treatments of Rh metal. Arrows indicate several 100 Å particles which have disappeared. (c), (d) Microstructure of oxidized Rh on SiO<sub>2</sub> after heating in NO at temperatures indicated. Shells form around particles similar to Rh metal.

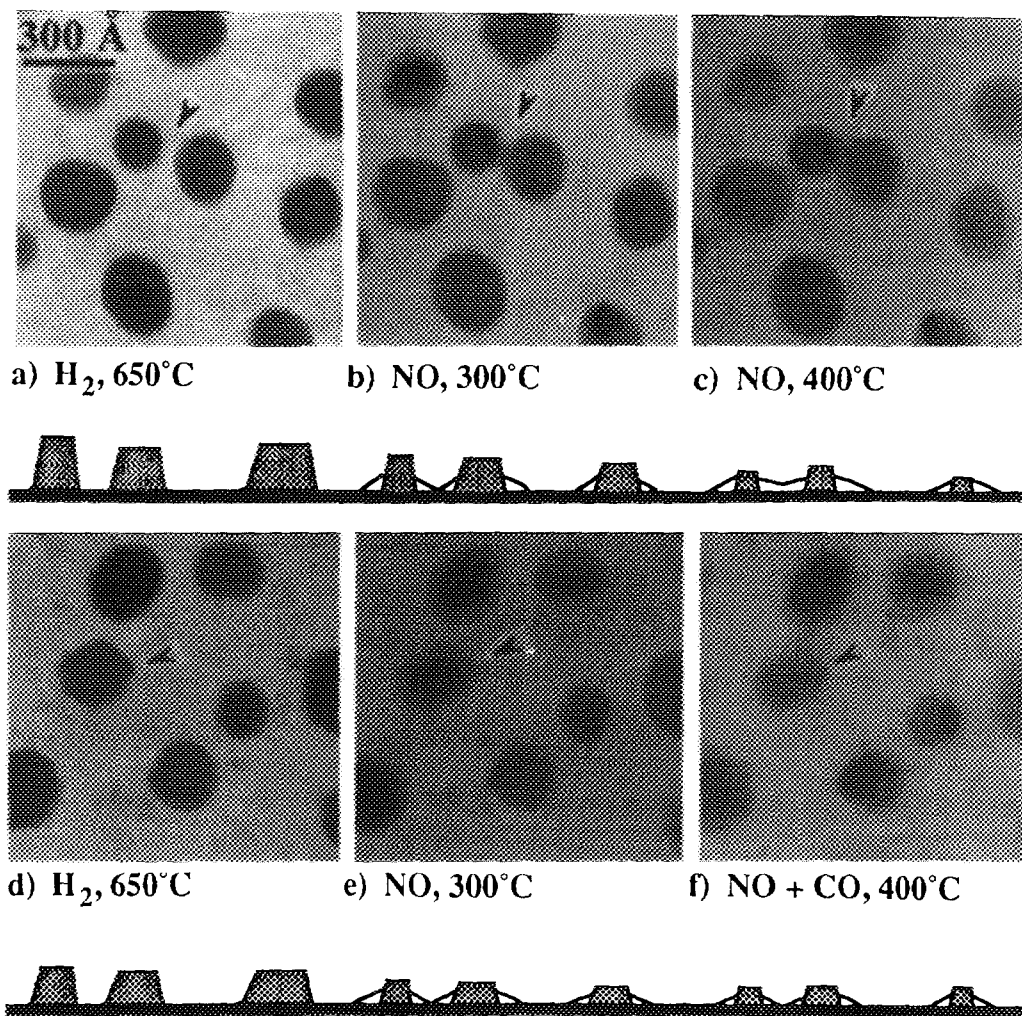


FIG. 3. (a)–(c) Microstructure after heating in NO. Shells form around Rh particles, arrows indicate area with substantial Rh dispersion. (d)–(f) Microstructure after heating in NO followed by NO + CO. Shells and Rh cores formed by heating in NO shrunk after heating in NO + CO.

3b and 3c after successive treatments in NO at 300°C for 30 hr and at 400°C for 10 additional hr. Even after treatment at 300°C, a low-contrast shell has formed around the perimeters of all the particles, and the shells of the adjacent particles in the center have intersected (indicated by arrows). The shells are  $\sim 20$  Å wide. After further heating in NO, the shells have grown to  $\sim 80$  Å in width and most of the high contrast cores have shrunk significantly. The Rh is being dispersed on the  $\text{SiO}_2$ , as evidenced by the in-

creased overlap of the shells of the adjacent particles. Only Rh metal was detected by electron diffraction after each treatment. The high contrast Rh metal particles reform after heating in  $\text{H}_2$ , indicating that significant volatilization has not occurred. Thus treatment in NO, even at temperatures as low as 300°C, disperses Rh particles on  $\text{SiO}_2$ .

The effects of NO treatment on oxidized Rh are shown in Figs. 2c and d. After heating in  $\text{O}_2$  at 600°C for 4 hr, Rh has been com-

pletely oxidized to  $\text{Rh}_2\text{O}_3$  as expected (Fig. 2c). Treatment in NO at  $400^\circ\text{C}$  for 10 hr produced significant dispersion of the Rh, as evidenced by the poorly defined edges of the particles and their reduced contrast in Fig. 2d. Further treatments indicate that the rate of Rh dispersion by heating in NO is comparable for previously oxidized and reduced Rh.

*NO followed by CO.* The effects of treatment in NO followed by treatment in CO were also studied (micrographs not shown). Low contrast shells  $\sim 50$  Å in diameter formed around the particles after heating in NO at  $500^\circ\text{C}$  for 10 hr. The size of the Rh cores decreased as the Rh is dispersed over the support by NO treatment as discussed above. After heating in CO at  $300^\circ\text{C}$  for 10 hr, the shells disappeared or shrunk, while their Rh cores were unaffected. The Rh particles have shrunk after successive treatments in NO and CO.

*NO followed by NO + CO.* Figure 3d shows Rh particles on another sample after heating in  $\text{H}_2$  at  $650^\circ\text{C}$  for 10 hr. Shells about 50 Å in diameter formed around the particles after heating in NO at  $300^\circ\text{C}$  for 30 hr and at  $400^\circ\text{C}$  for 10 additional hr (Fig. 3e). Figure 3f shows that after heating in NO + CO at  $300^\circ\text{C}$  for 10 hr, most of the shells have disappeared, but the Rh cores have continued to shrink. This contrasts with the microstructure observed after heating in NO followed by CO only described above, where the shells disappeared but the cores were unchanged or even grew slightly.

#### *Rh/Ce on $\text{SiO}_2$*

*NO + CO.* The microstructure of Rh/Ce on  $\text{SiO}_2$  after heating in NO + CO at  $300^\circ\text{C}$  is shown in Fig. 4. The region shown is on the same grid as the Rh only region shown in Fig. 1 and has undergone exactly the same heat treatments. After initial  $\text{H}_2$  treatment at  $650^\circ\text{C}$  for 10 hr, highly defected Rh particles are observed. The Ce is present as a  $\text{Ce}^{+3}$  film wetting the silica as we have characterized previously (5). Heating in NO +

CO for 20 hr has much less effect on Rh/Ce than on Rh only. The smaller Rh particles are still present in Fig. 4b and most of the larger particles have not changed significantly. A few of the larger particles have formed small regions of very high contrast within their interiors, two such examples are indicated by the arrows. Treatment for 10 additional hr (Fig. 4c) resulted in the formation of craters from the disappearance of these dark regions, but most of the particles are still unchanged. This treatment caused nearly complete loss of Rh in samples without Ce (Fig. 1), but even the smaller particles remain when Ce is present. Ce apparently masks most of the Rh particles, except the larger ones where the dark regions can form in exposed areas. The perimeters of the Rh particles, even those which lost significant Rh from their interiors, are largely unchanged. Heating in  $\text{H}_2$  caused the larger particles which lost Rh to sinter into smaller particles, while many of the smaller particles which lost Rh have broken into two even smaller particles (most easily seen in the upper right of Fig. 4d). Except for the particles which formed craters, the Rh loading appears comparable to that after the initial  $\text{H}_2$  treatment.

A much larger effect was observed when oxidized Rh/Ce was heated in NO + CO. Fig. 5a shows a region after heating in  $\text{O}_2$  at  $600^\circ\text{C}$  for 4 hr. As reported previously (4) the Ce coalesces from a film into crystalline  $\text{CeO}_2$  particles, uncovering much of the Rh. Heating this sample in NO + CO at  $300^\circ\text{C}$  for 24 hr (Fig. 5b) caused significant loss of Rh from all of the particles, but the Rh appears to have volatilized without forming a dispersed film. This can be seen for two particles indicated by arrows in the figures. These particles have receded from the surrounding  $\text{CeO}_2$ , exposing the  $\text{SiO}_2$ . All of the Rh particles have well-defined edges and little evidence of a shell is observed, contrasting with the shells observed in samples without Ce.

*NO only, NO followed by NO + CO.* The



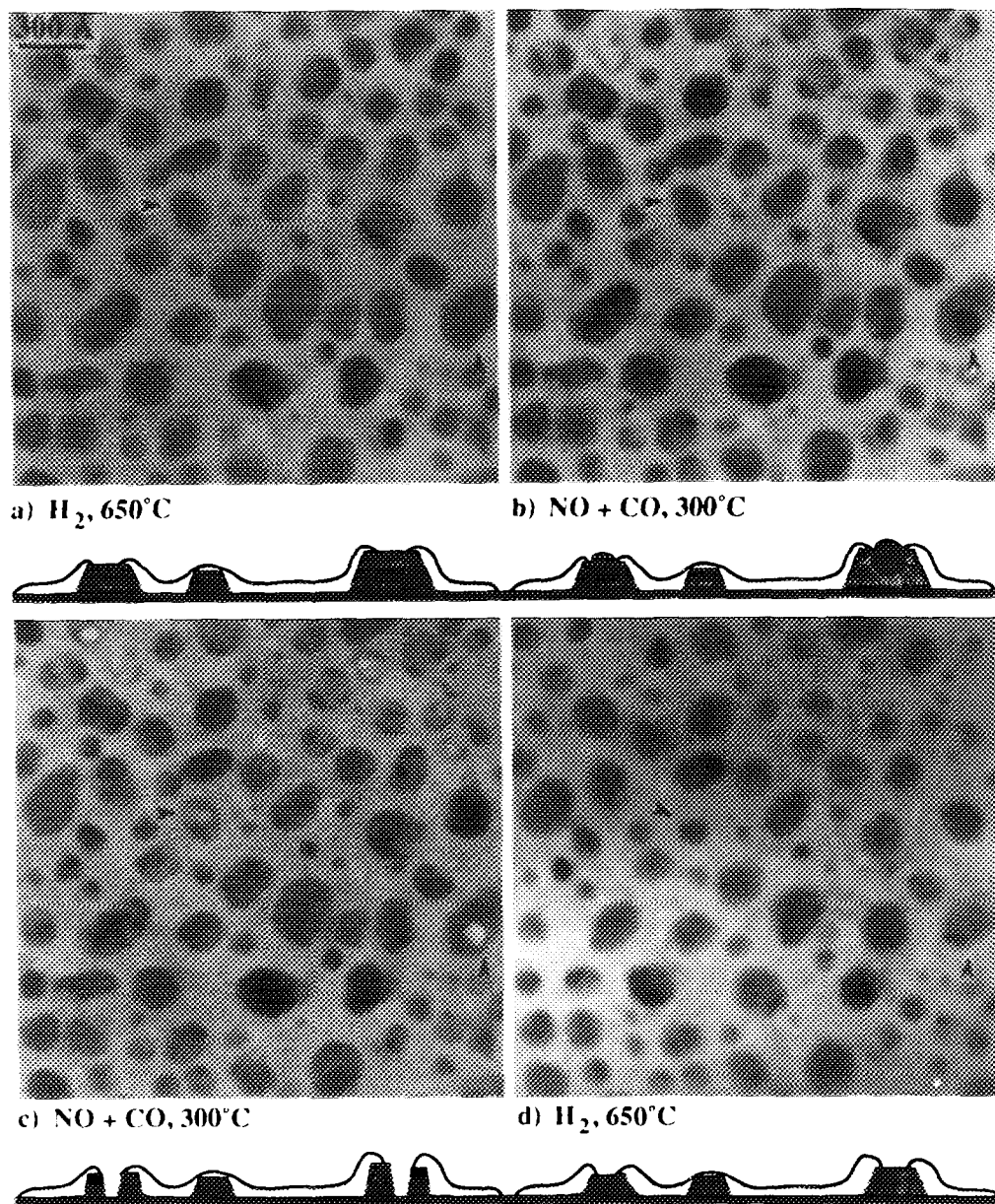


FIG. 4. Microstructure of Rh/Ce on  $\text{SiO}_2$  after heating in NO + CO at temperatures indicated. Disappearance of Rh is hindered by the addition of Ce. Arrows indicate two particles which lose Rh from their interiors.

effects of these treatments on Rh/Ce are shown in Fig. 6. The Ce film, present in a higher loading than in Fig. 4, formed an interconnected island structure on the  $\text{SiO}_2$  and Rh formed  $\sim 200$  Å diameter particles

on top of the Ce structures after initial  $\text{H}_2$  treatment at  $650^\circ\text{C}$  for 10 hr (Fig. 6a). Heating in NO at  $400^\circ\text{C}$  for 10 hr (Fig. 6b) and 20 additional hr (Fig. 6c) caused the Rh particles to disperse similar to samples without



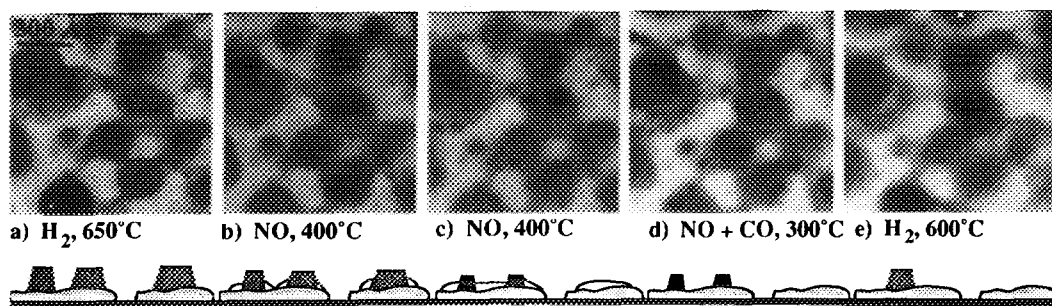


FIG. 5. (a), (b) Microstructure of oxidized Rh/Ce on  $\text{SiO}_2$  after heating in NO + CO at temperature indicated. Rh disappearance was greater than on reduced Rh/Ce; arrows indicate two particles which lost significant Rh after this treatment. (c), (d) Microstructure of oxidized Rh/Ce after heating in NO. Some Rh dispersion is observed similar to reduced Rh/Ce.

Ce. Little change is observed in areas of the  $\text{SiO}_2$  not covered by Ce islands, indicating that the Rh appears to disperse preferentially on the Ce. Heating in NO + CO at  $300^\circ\text{C}$  for 10 hr (Fig. 6d) caused some loss of contrast from the dispersed Rh, indicating that some volatilization has occurred. A few Rh particles return after heating in  $\text{H}_2$  at  $600^\circ\text{C}$  for 10 hr (Fig. 6e), but many do not, further indicating that Rh was lost during the NO + CO treatment.

Oxidized Rh appears to be less easily dispersed by treatment in NO when Ce is present. Figures 5c and d show the microstructure of Rh/Ce after heating in  $\text{O}_2$  at  $600^\circ\text{C}$  for 4 hr and in NO at  $400^\circ\text{C}$  for 10 hr, respectively. This sample has a lower Ce loading than the sample discussed above. Heating in  $\text{O}_2$  oxidized the Rh to  $\text{Rh}_2\text{O}_3$  and the Ce to  $\text{CeO}_2$ , as expected (Fig. 5c). Most of the Rh has been exposed by the coalescence of the Ce film into  $\text{CeO}_2$  particles, but treatment in NO resulted in only slight dispersion of the Rh.

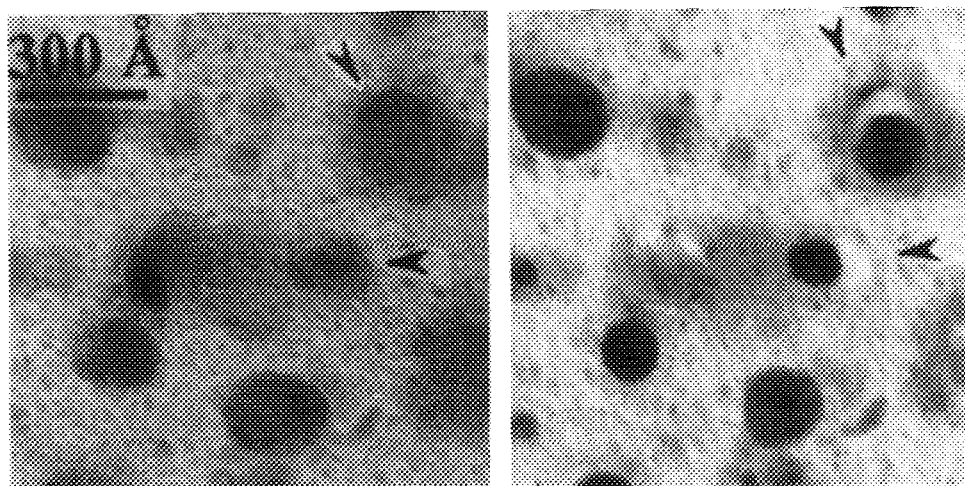
*CO only.* Heating for long times in CO at temperatures up to  $400^\circ\text{C}$  caused insignificant change in the microstructure of Rh/Ce on  $\text{SiO}_2$  (not shown). This is the same result observed for treatment of Rh only in  $\text{SiO}_2$ .

#### XPS on $\text{SiO}_2$

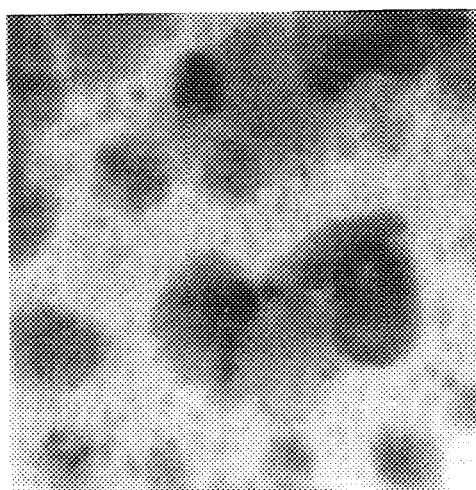
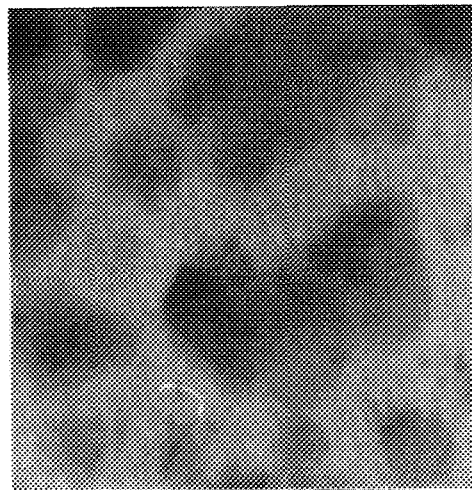
XPS of samples heated in NO + CO at  $300^\circ\text{C}$  indicate the formation of  $\text{Rh}^{+3}$  and

the oxidation of  $\text{Ce}^{+3}$  to  $\text{Ce}^{+4}$ . Figure 7 shows Rh  $3d$  XPS spectra from (a)  $20 \text{ \AA}$  Rh alone, (b)  $20 \text{ \AA}$  Rh/ $50\text{-\AA}$  Ce, and (c)  $20 \text{ \AA}$  Rh/ $140 \text{ \AA}$  Ce after heating in  $\text{H}_2$  at  $600^\circ\text{C}$  for 4 hr, NO + CO for 10 hr, and NO + CO for 10 additional hr. Spectra of Rh alone show no evidence of oxide, only a doublet from  $\text{Rh}^0$  (Rh  $3d_{5/2}$  at  $307.4 \text{ eV}$ ). The  $\text{Rh}_2\text{O}_3$  doublet (Rh  $3d_{5/2}$  at  $309.5 \text{ eV}$ ) was detected after Ce addition, particularly for the highest loading. The intensity of the Rh signal was attenuated by a factor of  $\sim 10$  after addition of  $140 \text{ \AA}$  Ce. The same results were observed in spectra from samples treated in NO (not shown).

We believe that Ce partially covers the Rh, thus attenuating the signal from bulk Rh particles and enhancing detectability of any nonzero-valent surface species formed during treatment in NO + CO. However, assignment of the shifted Rh peaks as the dispersed Rh phase is unclear for several reasons. First, the signal may be from the oxidized surface of Rh particles themselves. Second, the shifted peaks appear in Rh/Ce samples only and Ce may play a role in their formation. Recall from Fig. 4 that Rh disappearance was strongly hindered by the presence of Ce. Finally, the oxidation behavior of Rh in a moderate temperature NO + CO mixture will depend on temperature and gas composition, and additional experiments in this area may be interesting.

a) O<sub>2</sub>, 600°C

b) NO + CO, 300°C

c) O<sub>2</sub>, 600°C

d) NO, 400°C



FIG. 6. Microstructure of Rh/Ce on SiO<sub>2</sub> after treatments indicated. Rh particles are dispersed on the thick Ce island structure by heating in NO. Some Rh is volatilized by heating in NO + CO, as evidenced by the absence of Rh particles after reduction.

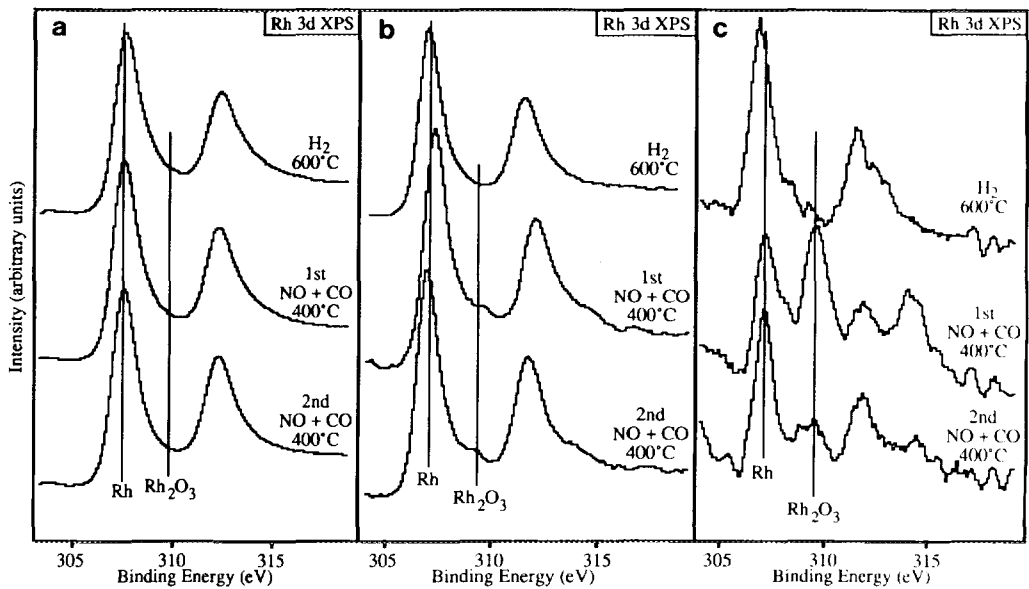


FIG. 7. Rh 3d XPS spectra of (a) 20 Å Rh, (b) 20 Å Rh/50 Å Ce, and (c) 20 Å Rh/140 Å Ce on SiO<sub>2</sub> after treatments indicated.

Ce 3d XPS spectra are shown in Fig. 8. After heating in H<sub>2</sub>, Ce is present in a mixture of +3 and +4 valence states. After

heating in NO + CO, the ratio of Ce<sup>+4</sup>/Ce<sup>+3</sup> increased, indicating oxidation of Ce under these conditions.

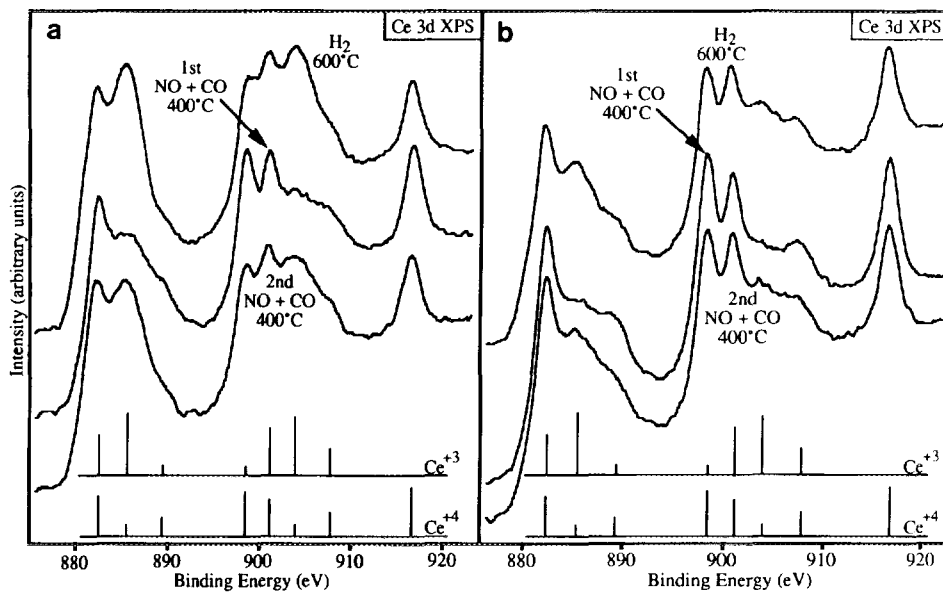


FIG. 8. Ce 3d XPS spectra of (a) 20 Å Rh/50 Å Ce and (b) 20 Å Rh/140 Å Ce on SiO<sub>2</sub> after treatments indicated.

*Rh and Rh/Ce on Al<sub>2</sub>O<sub>3</sub>*

*NO + CO.* Figure 9 shows the microstructure of Rh on Al<sub>2</sub>O<sub>3</sub> before and after extensive treatments in NO + CO. Rh parti-

cles formed after initial H<sub>2</sub> treatment at 650°C for 10 hr are 100–200 Å in diameter (Fig. 9a). Very little change was observed after heating in NO + CO at 300°C for 24 hr (Fig. 9b) and at 400°C for 10 additional hr

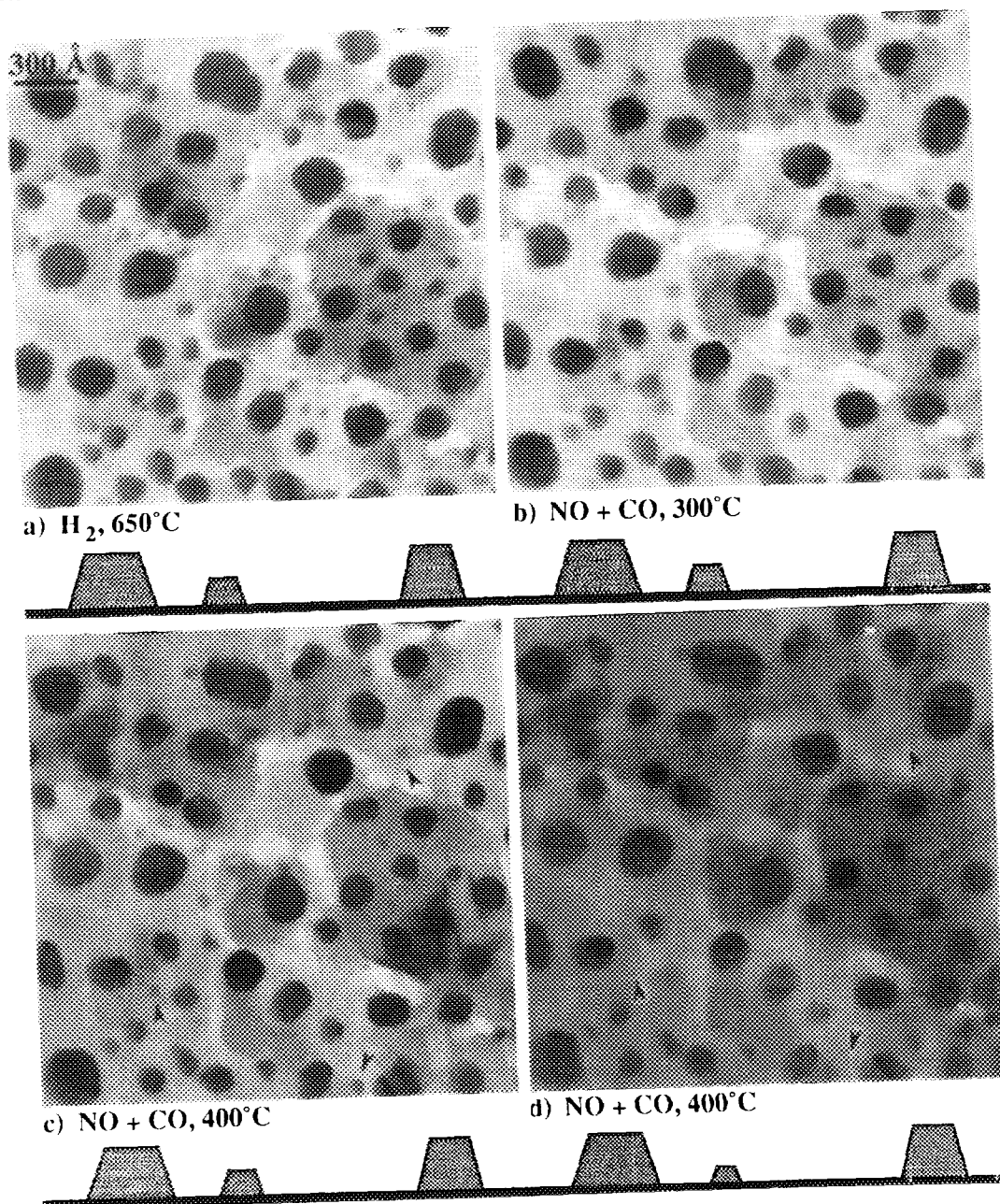


FIG. 9. Microstructure of Rh on Al<sub>2</sub>O<sub>3</sub> after heating in NO + CO at temperatures indicated. No changes in microstructure are observed until the final treatment, where several smaller particles (indicated by arrows) have disappeared.

(Fig. 9c). Note that these treatments caused nearly complete loss of Rh supported on  $\text{SiO}_2$  (Fig. 1). A few smaller particles, indicated by the arrows in Fig. 9d, have finally disappeared after heating at  $400^\circ\text{C}$  for another 10 hr, but Rh loss does not occur to a significant extent on alumina.

Rh also does not detectably disappear from samples with Ce on  $\text{Al}_2\text{O}_3$ . Figures 10a–10c show the microstructure of the same Rh/Ce region after heating in  $\text{H}_2$  at  $650^\circ\text{C}$  for 10 hr and after heating in  $\text{NO} + \text{CO}$  at  $400^\circ\text{C}$  for 28 hr and 38 additional hr, respectively. The Ce is present as  $\text{CeO}_2$  even after heating in  $\text{H}_2$ , as reported previously (6), and the Rh forms larger particles than without Ce. Two Rh particles are indicated by arrows in the figures. The smaller particles are crystalline  $\text{CeO}_2$  which can be observed on both the  $\text{Al}_2\text{O}_3$  and on the Rh particles. Treatment in  $\text{NO} + \text{CO}$  causes very little change in the Rh particles, but several of the  $\text{CeO}_2$  particles have disappeared and several new ones have formed, indicating that this treatment causes some changes in Ce oxidation states as observed with XPS.

*NO only, NO followed by CO.* Heating in

$\text{NO}$  did produce significant changes in the microstructure of both Rh and Rh/Ce on  $\text{Al}_2\text{O}_3$ . Figure 11 shows the interface between Rh only and Rh/Ce regions prepared on the same grid by shielding the area in the left side of the figure during the Ce evaporation. This sample has a large Ce loading ( $\text{Ce}/\text{Rh} \sim 3$ ). The sample was prepared from a single Rh evaporation, deposited before the Ce, therefore the Rh loadings are identical in both the Rh and Rh/Ce regions. The interface between no Ce and full Ce loading is  $\sim 2000 \text{ \AA}$  wide. The figure shows the microstructure after initial heating in  $\text{H}_2$  at  $650^\circ\text{C}$  for 10 hr (Fig. 11a), after heating in  $\text{NO}$  at  $400^\circ\text{C}$  for 40 hr (Fig. 11b), and after heating in  $\text{CO}$  at  $400^\circ\text{C}$  for 40 more hr (Fig. 11c).

Heating in  $\text{NO}$  caused the formation of small ( $< \sim 30 \text{ \AA}$ ) Rh particles from the edges of the original particles. The particles were observed in both the Rh and Rh/Ce regions and are most prevalent near large Rh particles. A shell, surrounded by a ring of small particles, is observed around the large Rh particles, which have decreased in size. The diameter of the shell and Rh core is the same as that of the initial Rh particle. The remarkable changes in microstructure observed

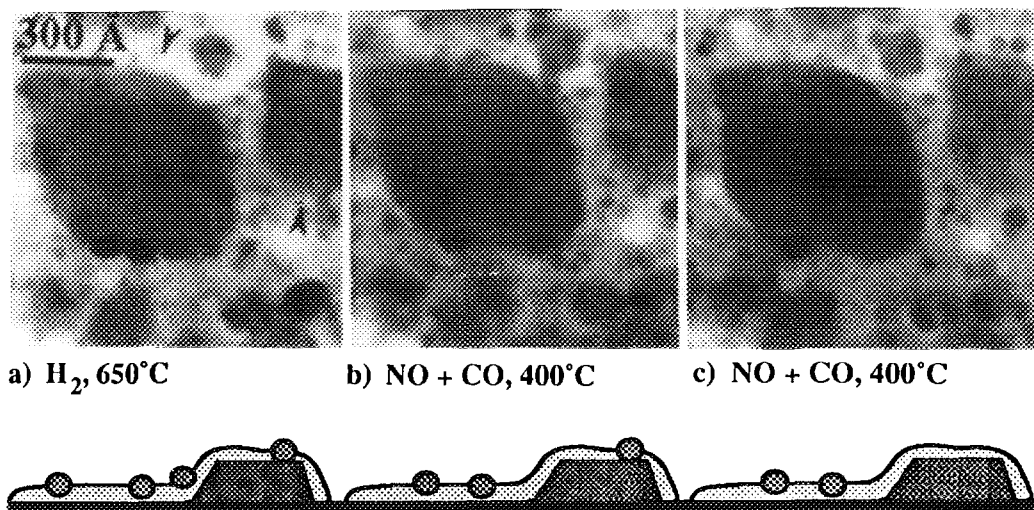


FIG. 10. Microstructure of Rh/Ce on  $\text{Al}_2\text{O}_3$  after heating in  $\text{NO} + \text{CO}$  at temperatures indicated. No changes in Rh particles, indicated by arrows, were observed, although some changes did occur in the small  $\text{CeO}_2$  particles.

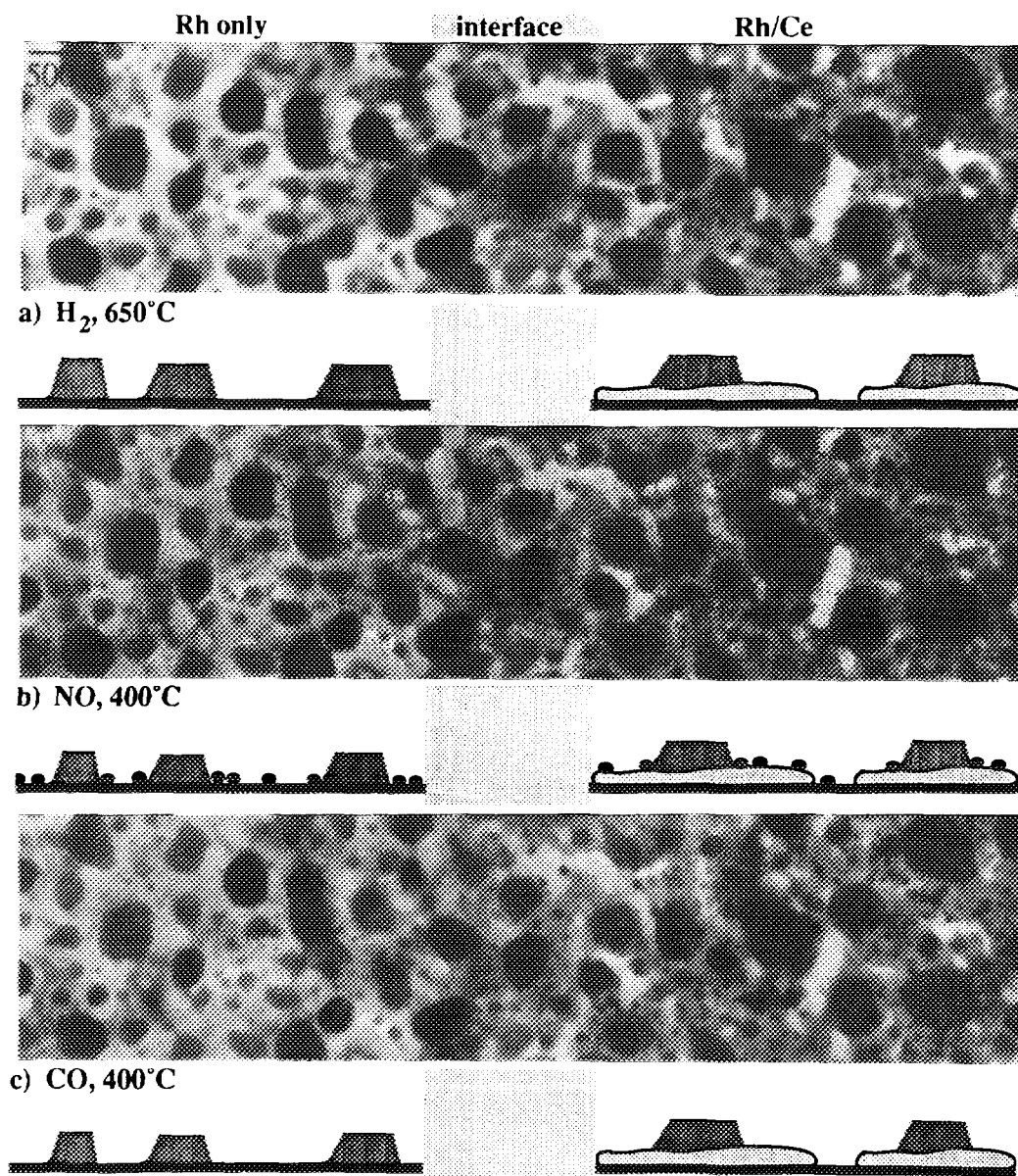


FIG. 11. Microstructure of Rh and Rh/Ce on  $\text{Al}_2\text{O}_3$  after heating in NO followed by CO at temperatures indicated. Many small Rh particles formed from the edges of Rh particles in both regions by heating in NO. These particles disappeared after heating in CO, mostly by sintering back into the larger particles.

after heating in NO are in strong contrast to the lack of changes observed after heating  $\text{Al}_2\text{O}_3$  supported Rh in NO + CO.

Heating in CO caused the disappearance of the dispersed Rh particles and the shells from both regions of the sample. Some of

the Rh appears to have sintered back into large Rh particles, but many of the particles are now slightly smaller than after the initial  $\text{H}_2$  treatment. It is difficult to ascertain whether any Rh has been volatilized by this NO  $\rightarrow$  CO cycle.

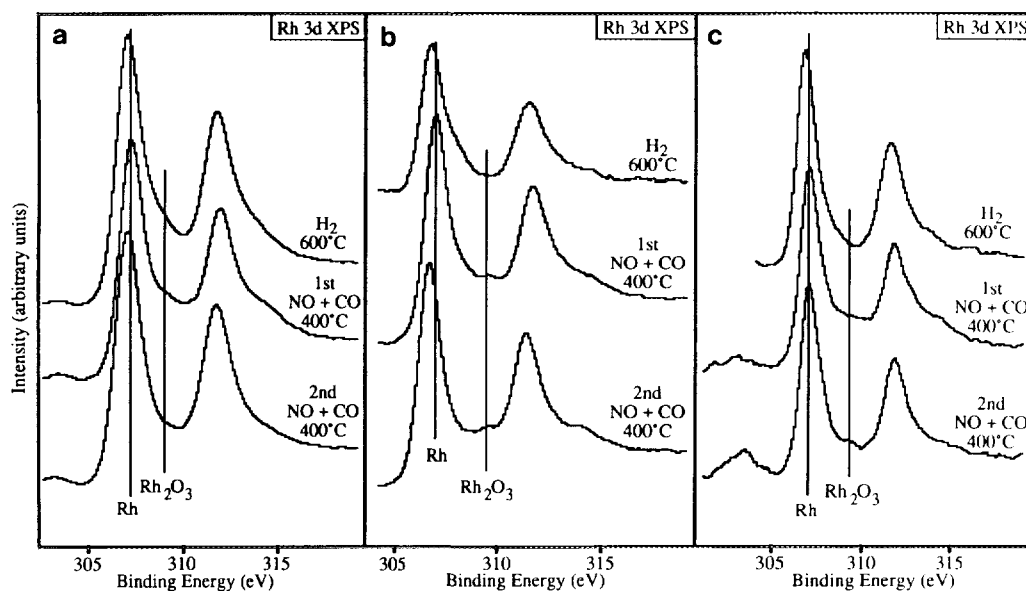


FIG. 12. Rh 3d XPS spectra of (a) 20 Å Rh, (b) 20 Å Rh/50-Å Ce, and (c) 20 Å Rh/140 Å Ce on  $\text{Al}_2\text{O}_3$  after treatments indicated.

### XPS on $\text{Al}_2\text{O}_3$

Rh 3d XPS spectra are shown in Figs. 12a–12c for 20 Å Rh, 20 Å Rh/50-Å Ce, and 20 Å Rh/140 Å Ce on alumina, respectively,

after heating in  $\text{H}_2$  at 600°C for 4 hr and two successive heatings in NO + CO at 300°C for 10 hr each. Only  $\text{Rh}^0$  is observed in the sample without Ce. In contrast with the results on  $\text{SiO}_2$ , very little evidence of Rh

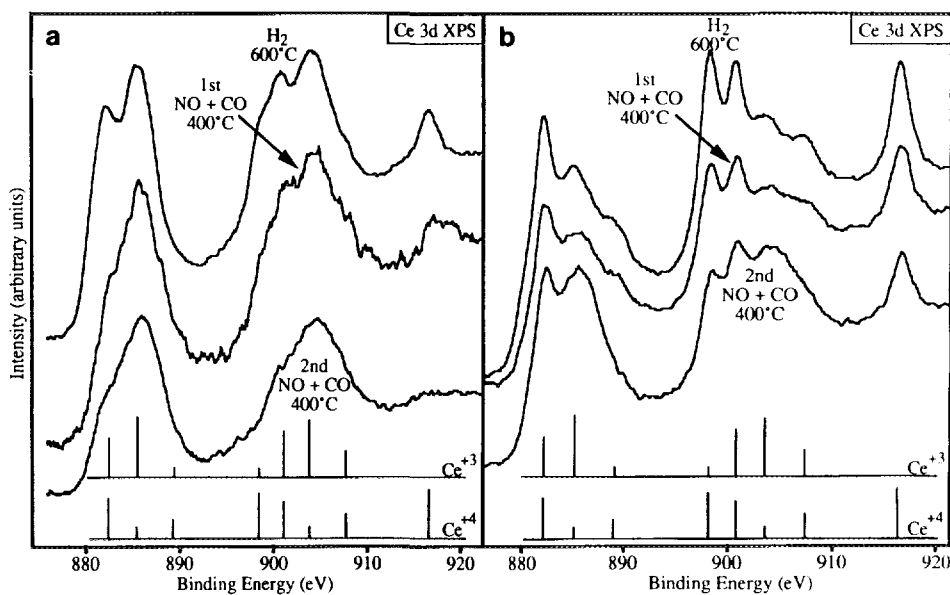


FIG. 13. Ce 3d XPS spectra of (a) 20 Å Rh/50 Å Ce and (b) 20 Å Rh/140 Å Ce on  $\text{Al}_2\text{O}_3$  after treatments indicated.



oxide formation is observed after Ce addition, even for the highest Ce loading. The same results were obtained when samples were treated in NO alone (spectra not shown). Ce 3d XPS spectra (Fig. 13) also show a different effect than on SiO<sub>2</sub>. Initially present as mostly Ce<sup>+4</sup>, the Ce is reduced to predominantly Ce<sup>+3</sup> after heating in NO + CO, indicating that Ce is providing oxygen storage. This result is interesting since previous work has shown that CeO<sub>2</sub> on Al<sub>2</sub>O<sub>3</sub> is not reduced by treatment in H<sub>2</sub> (6). As discussed previously, the effects of temperature and gas composition on Rh behavior may be an interesting area for further study.

#### REACTIVITY

##### Rh on SiO<sub>2</sub>

The activity of 5% Rh/SiO<sub>2</sub> reduced in H<sub>2</sub> at 650°C for 4 hr for reaction of 5% NO + 5% CO was examined to determine the effect on reactivity of the dramatic microstructural changes observed with TEM (Fig. 14a). Insignificant activity was observed below 200°C. NO and CO conversions at 200°C were 10 and 7%, respectively, and N<sub>2</sub> selectivity, defined as mol N<sub>2</sub>/(mole N<sub>2</sub> + mole N<sub>2</sub>O), was about 30%. No changes in reactivity were observed while heating at 200°C overnight. The temperature was then increased to 300°C for 15 hr, similar to the TEM treatments, and 100% conversions and 50% N<sub>2</sub> selectivity were measured. After treating the catalyst at 300°C, the temperature was lowered to 200°C and activity measured again over a period of ~10 hr. As shown in Fig. 14a, the activity decreased by a factor of five compared to the original activity at 200°C. Thus, treatment at 300°C in NO + CO caused significant *deactivation* of the catalyst, as would be expected from the TEM results, while N<sub>2</sub> selectivity remained at ~30%.

##### Rh on Al<sub>2</sub>O<sub>3</sub>

Results from the same experiment using a freshly calcined 5% Rh/Al<sub>2</sub>O<sub>3</sub> catalyst are shown in Fig. 14b. NO and CO conversions

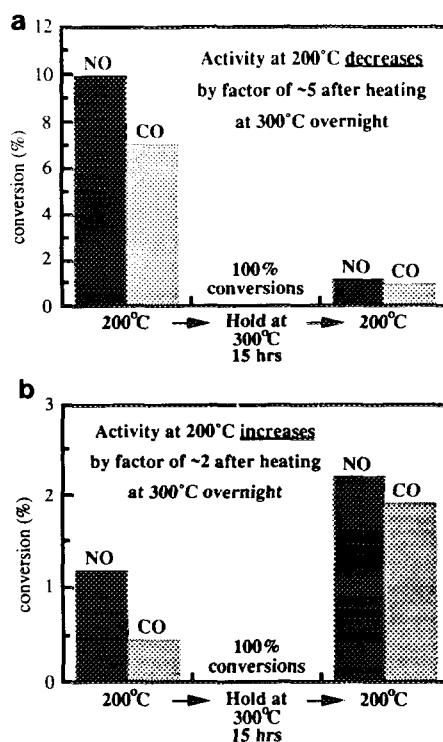


FIG. 14. Effects of treatment in NO + CO on reactivity of Rh on (a) SiO<sub>2</sub> and (b) Al<sub>2</sub>O<sub>3</sub>. Activity was measured at 200°C, catalysts aged overnight in NO + CO at 300°C, and activity measured again at 200°C.

were less than 2% at 200°C and increased to 100% at 300°C. N<sub>2</sub> selectivity was about 20% at 200°C and increased to 65% at 300°C. After heating overnight at 300°C, the activity actually improved slightly, by a factor of ~2, consistent with the lack of Rh disappearance observed with TEM and N<sub>2</sub> selectivity remained at 20%.

#### DISCUSSION

The microstructures of Rh on SiO<sub>2</sub> and Al<sub>2</sub>O<sub>3</sub> in NO + CO are summarized schematically in Fig. 15. On SiO<sub>2</sub>, heating in NO + CO causes both the dispersion and volatilization of 100–200 Å diameter Rh particles. Subsequent treatment in H<sub>2</sub> sinters any remaining Rh into small particles. The loss of Rh is a combined effect of heating in NO + CO: heating in NO disperses the Rh particles and subsequent heating in CO vola-

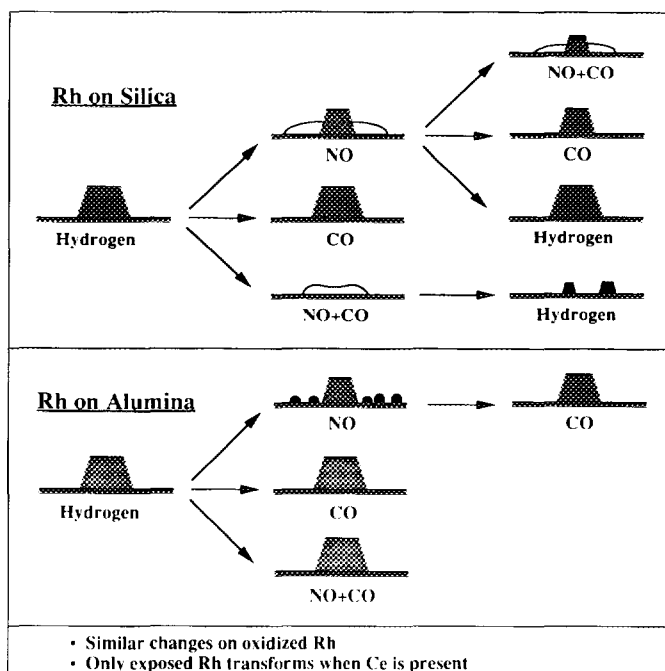


FIG. 15. Schematic of microstructural changes observed during treatments in NO + CO, NO, and CO.

tilizes the dispersed Rh. No change in microstructure is observed when undispersed Rh particles are heated in CO only. Preoxidized  $\text{Rh}_2\text{O}_3$  particles are more susceptible to volatilization in NO + CO than Rh metal, suggesting that dispersion of reduced Rh may involve oxidation as suggested by XPS. The addition of Ce appears to inhibit Rh loss by covering the particles; much less Rh is lost after identical treatments from Rh/Ce regions on the same grid as Rh only regions.

We are unable to characterize the dispersed Rh phase produced by treatments in NO and NO + CO, but we speculate that it involves a highly mobile Rh nitrosyl compound. Observed dispersion in the absence of CO eliminates the possibility of mixed Rh-C/N species such as isocyanate or cyanide. Rh nitrosyls are known to form on silica at these temperatures (13, 15, 16) and the addition of NO has been shown to greatly enhance the rate of CO-induced oxidative disruption of small Rh clusters below

100°C (13). The observation with XPS of Rh binding energies similar to  $\text{Rh}^{-3}$  is consistent with this suggestion; carbonyls and nitrosyls with formal charges of only +1 show Rh  $3d_{5/2}$  binding energies in the range expected for  $\text{Rh}_2\text{O}_3$  (17). Another possibility is that Rh-NO complex present in the dispersed phase is transformed to  $\text{Rh}_2\text{O}_3$  by exposure to room temperature air.

Volatilization of Rh occurs in CO only, but only for Rh previously dispersed by NO. Treatments in NO or treatments of undispersed Rh particles in CO do not cause Rh loss. This strongly suggests that volatilization occurs by formation of a carbonyl with a small number of Rh atoms, possibly  $\text{Rh}_4(\text{CO})_{12}$  or  $\text{Rh}_6(\text{CO})_{16}$ . These have sufficient stability and vapor pressure to be used for preparation of Rh catalysts (18). The interaction between Rh in the dispersed phase and the  $\text{SiO}_2$  support is apparently weak enough to permit volatilization under these conditions, but probably not on  $\text{Al}_2\text{O}_3$ .

Heating in NO + CO has less obvious effects on the microstructures of Rh and Rh/Ce on Al<sub>2</sub>O<sub>3</sub>; Rh particles are not dispersed in this mixture as observed on SiO<sub>2</sub>. Heating in NO only, however, does disperse Rh particles into very small (~20-Å diameter) particles which may form from a dispersed film upon exposure to room temperature air. This is observed for both Rh only and Rh/Ce. Heating this dispersed Rh in CO results primarily in sintering back to larger particles, although some volatilization may occur.

Reactivity measurements correlated well with TEM observations. NO + CO activity on SiO<sub>2</sub> decreased by a factor of five when the catalyst was heated overnight at 300°C, as would be expected if significant Rh loss occurred. The decrease in activity is not as large as TEM observations may suggest because volatilized Rh can redeposit on nearby SiO<sub>2</sub> in the porous supported catalyst powder. On Al<sub>2</sub>O<sub>3</sub>, a slight increase in activity was seen for the same catalyst treatment, consistent with the absence of significant volatilization but some dispersion observed with TEM.

The obvious differences in microstructure on the two supports suggest differences in their interactions with Rh and with NO and CO. Heating in NO only did disperse Rh on Al<sub>2</sub>O<sub>3</sub>, but small particles were observed instead of the film seen on SiO<sub>2</sub> after the same treatment. It may be that a film formed under NO, but transformed into energetically favorable small Rh crystals upon exposure to air. These crystals are probably too large to be volatilized and subsequent heating in CO simply resulted in sintering back to larger particles. This explanation does not, however, account for the lack of change when Rh on Al<sub>2</sub>O<sub>3</sub> is heated in NO + CO. We suggest that CO-induced reduction and/or sintering may be much faster on Al<sub>2</sub>O<sub>3</sub> than on SiO<sub>2</sub>, thereby inhibiting dispersion of Rh by NO.

The particles studied in this work are much larger than the clusters used to study CO induced disruption by IR described pre-

viously (19). We would not be able to observe 15–20 atom clusters with TEM, and therefore are unable to directly observe this phenomenon. However, we can discount the formation of such clusters as the source of Rh disappearance since, if they did not volatilize, they would be expected to easily sinter into particles upon heating in H<sub>2</sub>.

#### SUMMARY

Silica supported Rh is dispersed and volatilized by low temperature treatment in NO + CO. Treatment in NO alone disperses Rh particles and subsequent treatment in CO alone volatilizes the dispersed Rh, although heating in CO alone has no effect on undispersed Rh. Preoxidation increases Rh disappearance, but Ce addition hinders Rh loss. The activity of Rh on SiO<sub>2</sub> for NO + CO at 200°C decreased by a factor of 5 after heating overnight at 300°C, as expected if Rh is lost from the catalyst.

On alumina, only a few small Rh particles disappeared even after extensive treatment in NO + CO, although heating in NO alone did disperse the Rh into small (~20 Å) particles on the Al<sub>2</sub>O<sub>3</sub>. Subsequent treatment in CO resulted primarily in sintering of the dispersed particles. NO + CO activity on alumina actually increased slightly by heating at 300°C for extended time, consistent with TEM observations.

It is important to note that these dramatic changes in microstructure occur under conditions that would be regarded as mild for a working catalyst. Conventional wisdom suggests that Rh is not mobile at 300°C and certainly should not disappear under these conditions. The application of techniques sensitive to surface species should be useful in further characterizing the dispersed and volatile compounds.

#### REFERENCES

1. Oh, S. H., *J. Catal.* **124**, 477 (1990).
2. Klemmer, P. G., M.S. thesis, Brigham Young University, 1989.
3. Kiennemann, A., Breault, R., Hindermann, J.-P., and Laurin, M., *J. Chem. Soc. Faraday Trans. 1* **83**, 2119 (1987).

4. Chojnacki, T., Krause, K., and Schmidt, L. D., *J. Catal.* **128**, 161 (1991).
5. Krause, K. R., Schabes-Retchkiman, P. S., and Schmidt, L. D., *J. Catal.* **134**, 204 (1992); Krause, K. R., and Schmidt, L. D., *Catal. Lett.* **14**, 141 (1992).
6. Schwartz, J. M., and Schmidt, L. D., *J. Catal.*, **138**, 283 (1992).
7. Lee, C., and Schmidt, L. D., *J. Catal.* **101**, 123 (1986).
8. Yang, A. C., and Garland, C. W., *J. Phys. Chem.* **61**, 1504 (1957).
9. Solymosi, F., and Pásztor, M., *J. Phys. Chem.* **90**, 5312 (1986).
10. Basu, P., Panayotov, D., and Yates, J. T., Jr., *J. Phys. Chem.* **91**, 3133 (1987).
11. Van't Blik, H. F. J., van Zon, J. B. A. D., Huijzinga, T., Vis, J. C., Koningsberger, D. C., and Prins, R., *J. Am. Chem. Soc.* **107**, 3139 (1985).
12. Buchanan, D. A., Hernandez, M. E., Solymosi, F., and White, J. M., *J. Catal.* **125**, 456 (1990).
13. Solymosi, F., Bãnsági, T., and Novák, E., *J. Catal.* **112**, 183 (1988).
14. Solymosi, F., Pásztor, M., and Rákhely, G., *J. Catal.* **110**, 413 (1988).
15. Hyde, E. A., Reedham, R., and Rochester, C. H., *J. Chem. Soc. Faraday Trans. 1* **80**, 531 (1984).
16. Arai, H., and Tominaga, H., *J. Catal.* **43**, 131 (1976).
17. Cannon, K. C., and White, J. M., *J. Catal.* **120**, 314 (1989).
18. Frederick, B. G., Apai, G., and Rhodin, T. N., *J. Am. Chem. Soc.* **109**, 4797 (1987).
19. Solymosi, F., and Pásztor, M., *J. Phys. Chem.* **89**, 4789 (1985).